Oil & Gas Science and Technology – Rev. IFP, Vol. 57 (2002), No. 1, pp. 59-69

Vortex-Induced Vibrations of Risers: Theoretical, Numerical and Experimental Investigation

C. Le Cunff[1], F. Biolley[1], E. Fontaine[1], S. Étienne[2] and M.L. Facchinetti[3]

1 Institut français du pétrole, 1 et 4, avenue de Bois-Préau, 92852 Rueil-Malmaison Cedex - France
2 Département Génie mécanique, École polytechnique, 2500 Chemin de Polytechnique, H3T1J4 Montréal (QC) - Canada
3 École polytechnique, Laboratoire d'hydrodynamique, CNRS, 91128 Palaiseau Cedex - France
e-mail: cedric.le-cunff@ifp.fr - francis.biolley@ifp.fr - emmanuel.fontaine@ifp.fr - stephane.etienne@polymtl.ca - matteo@ladhyx.polytechnique.fr

Résumé — Vibrations d'un riser soumis à un écoulement : étude théorique, numérique et expérimentale — Les vibrations engendrées par le relâcher tourbillonnaire dans le sillage d'un cylindre soumis à un courant peuvent créer une fatigue importante dans les tubes utilisés par l'industrie offshore pour amener le pétrole ou le gaz du fond de la mer jusqu'à la plate-forme ou le navire de stockage. Ce sujet fait l'objet de très nombreuses études et, à l'*Institut français du pétrole*, plusieurs modèles sont développés pour prédire la durée de vie de ces tubes. Les méthodes vont d'une simple analyse modale de la réponse de la structure jusqu'à un calcul couplé fluide-structure avec résolution des équations de Navier-Stokes. Au travers du projet Hydlines, des campagnes d'essais sont menées pour valider les différentes approches.

Mots-clés : vibrations induites par vortex (VIV), riser, fatigue, offshore.

Abstract* — *Vortex-Induced Vibrations of Risers: Theoretical, Numerical and Experimental Investigation — *Vibrations due to vortex shedding in the wake of a cylinder exposed to a current can create fatigue damage in risers used by the offshore industry to bring oil and gas from the sea floor to the platform or off-loading vessel. Extensive research is conducted in this domain and at the* Institut français du pétrole, *several models are proposed to predict the fatigue life of such pipes. The methods range from simple modal calculations to fully coupled analysis of the fluid-structure interaction and resolution of the Navier-Stokes equations. Through the Hydlines Project, experiments are conducted to validate the various approaches.*

Keywords: vortex-induced vibrations (VIV), riser, fatigue, offshore.

INTRODUCTION

If a current impacts on a circular cylinder, fluctuating forces are created due to vortex-shedding in the wake. If the cylinder is mounted on springs, the forces induce a displacement of the structure, which in turn, modifies the flow, leading to a fully coupled fluid-structure interaction. The displacement of the cylinder under a current is referred to as a vortex-induced vibration (VIV). Much research is available on the subject and more details can be obtained in various books or reviews: Marris (1964), Sarpkaya (1979), Bearman (1984), Griffin (1985), Chen (1987), Blevins (1990), Sheppard and Omar (1992), Naudascher and Rockwell (1994), and Williamson (1996).

The industrial interest for VIV is based on the fatigue that a long cylindrical structure can experience. The main applications are chimneys and cables for bridges in air, and pipes, towing cables, and mooring lines in water. The focus of the present paper is the risers used in the offshore industry to carry oil from the bottom of the ocean to a floating facility. Reviews on the specifics of VIV in risers are given in Pantazopoulos (1998).

The fatigue due to VIV can be the dominant fatigue in some risers configurations. An example of well-head failure is provided by Hopper (1983). A drilling riser was installed in a depth of 1450 ft of water. Measurements of currents were performed during the drilling operation. A fatigue life estimate due to VIV was undertaken using these currents. Calculations predicted failure after 29 days, the actual in-service life being 27 days. The failure due to VIV was also confirmed by real time measurements of riser ball joint angle. With the arrival of deep and ultra-deep offshore field, and new configurations of riser (steel-catenary risers (SCR), hybrid risers, etc.), any design must now include an analysis of the fatigue due to VIV. If the damage is expected to be too great, anti-VIV devices are proposed. The most commonly-used are strakes installed along the pipe on the most exposed area. Others techniques can be found in Zdravkovich (1981), Every *et al.* (1982), and Bruschi *et al.* (1996).

In the present paper, a short review of the vortex shedding is presented. Then, several approaches are proposed to compute the fluid-structure interaction. The first approach is based on the modal response of the structure; such a method is widely used in the industry since it is fast and provides a simple lifetime estimate. The second, more detailed approach requires solving the structural equation in time together with an equation which models the fluid. The third approach involves the resolution of the full Navier-Stokes equations, instead of a simple fluid model equation. Finally, the results of a set of experiments on a cable with multiple diameters are described. They will provide benchmark cases to validate the different methods.

1 VORTEX-INDUCED VIBRATIONS

The VIV phenomenon depends on various parameters. For the fluid, the two main parameters are the Reynolds number *Re* and the Strouhal number *St* defined by:

$$Re = \frac{UD}{\nu} \quad \text{and} \quad St = \frac{f_v D}{U} \tag{1}$$

where U is the fluid velocity, D, the diameter of the cylinder, ν the kinematic viscosity and f_v the shedding frequency. The fluid-structure coupling is characterized by the reduced velocity U_r:

$$U_r = \frac{U}{f_m D} \tag{2}$$

where f_m is an eigenfrequency of the structure.

The shedding of the vortices is sketched in Figure 1. It creates forces both in the cross-wise and stream-wise directions. Studies (Naudascher, 1987; Vandiver, 1987; Torum *et al.*, 1996) show that the in-line vibrations are an order of magnitude smaller than the transverse vibrations. In-line vibrations can also occur by themselves and constitute a fatigue problem for the free-span length of pipes on the sea-floor. They are usually not a concern for risers since they appear at lower reduced velocity. Axial vibrations (Huse *et al.*, 1998) are a by-product of cross-flow vibrations and are observed when the axial deformation due to the cross-flow vibrations triggers a resonant axial mode.

The lock-in phenomenon occurs when f_v and f_m are close to each other, corresponding to $U_r \approx 1/St$. In this case, the shedding frequency becomes equal to the eigenfrequency of the structure. The vibration amplitude is then maximum, and the correlation between the excitation forces along the span increases dramatically. In any case, the amplitude of vibration is limited to the order of one diameter.

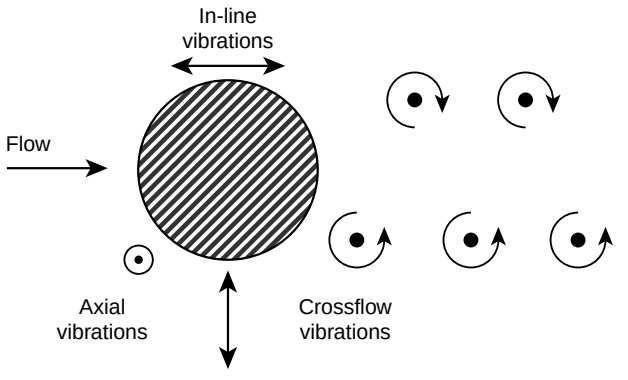

Figure 1

Vibrations of a cylinder submitted to vortex shedding.

2 MODAL APPROACH

The modal approach is described by various authors to compute the vibration amplitude of a structure (Iwan, 1981; Lyons and Patel, 1986; Moe, 1991; Bokaian, 1993; Nedergaard *et al.*, 1994). The first approximation usually assumes that the cross-flow displacements are the most dangerous, and restricts the analysis to the calculations of these displacements. The second approximation consists of calculating the fluid force on a given mode independently, neglecting the cross-interactions between the forces.

2.1 DeepVIV

DeepVIV is a module of the finite element code DeepLines (2000) which performs VIV calculations. The amplitude of vibration and the resulting fatigue are obtained based on a modal calculation of the response to a steady current. The structure is defined by elements: cable, bar or beam. A static analysis is first carried out to find the equilibrium position, followed by a modal analysis, and finally by VIV calculations. There is also the possibility of reading a pre-existing modal database, which is useful when a large number of modes is excited.

DeepVIV proceeds as follows:

– Calculations of the modes of the structure taking into account the external fluid displaced which is accomplished through an added mass coefficient.
– Selection of the potentially excited modes with two criteria:
  • the mode is mainly perpendicular to the flow and the structure (shape);
  • the frequency f satisfies the reduced velocity criterion: given St, the reduced velocity corresponding to St is $U_r = 1/St$, and the mode is excited if its frequency is located between $U_r - \Delta U_{\min}$ and $U_r + \Delta U_{\max}$. The lock-in area on the mode of frequency f_i is composed of all the points which satisfy the criterion. If more than one mode is selected, the mode with the frequency nearest to U_r is chosen.
– Calculation of the modal amplitude: a balance between the lift force and damping gives the amplitude of each mode. The lift can be reduced by taking into account an experimental correlation length. The hydrodynamic damping is based on Morison's formulation (1950) of the drag force, hence the use of a VIV drag coefficient. A "self-damping" is also implemented when the modal amplitude becomes higher than one diameter, which represents in the model the fact that VIV have a limited amplitude. The lift force is a function of both the amplitude and the Reynolds number. The lift coefficient has been validated through experimental results. Anti-VIV devices are modelled by a reduced lift coefficient.

The lift force is then applied on the structure and solved in the frequency domain on the modal basis of the structure. A classical fatigue analysis is performed based on Miner's rule (DNV, 1996), with the contribution of each load i to the bending stress (ΔS_i) and its period (T_i) to the damage given by:

$$D = \sum \frac{n_i}{N_i} = 365 * 24 * 3600 * \sum \frac{\Delta S_i^b}{CT_i} \tag{3}$$

The constant C and b are given by a fatigue curve:

$$N(\Delta S)^b = C \tag{4}$$

where N is the number of cycles to rupture under the stress range (ΔS). Rayleigh's correction, which is conservative, is also available, as well as Goodman's method (Lalanne, 1999) which takes into account the ratio of the static stress with respect to the yield stress.

2.2 Examples

2.2.1 Drilling Riser

A 790 m long riser is pinned at the seafloor and tensioned at the top. Seven areas of different hydrodynamic diameters, representing the buoyancy modules, are defined along the cable (from bottom to top) as indicated in Table 1.

TABLE 1

Variation of the diameter along the riser length from top to bottom. The length of the section and its diameter are provided

Length (m)	Diameter (m)
180.0	0.533
240.	1.12
15.0	1.12
70.0	1.17
135.0	0.533
125.0	1.00
25.0	0.533

TABLE 2

Variation of current velocity with depth

Depth (m)	Velocity (m/s)
0	0.4
100	0.5
200	0.5
300	0.2
400	0.3
500	0.4
900	0.4

The pipe itself has a constant diameter of 0.533 m with a thickness of 0.016 m. The top tension is equal to $3.25 \cdot 10^6$ N. The current perpendicular to the riser is defined as a function of depth *(Table 2)*.

For $St = 0.2$, the excited frequencies are summarized in Table 3 (obtained with an added mass coefficient of 1) .

TABLE 3

Excited eigenfrequencies of the riser

Mode	Frequency (Hz)
2	0.439E – 01
3	0.675E – 01
4	0.921E – 01
5	0.116E + 00
6	0.141E + 00
7	0.164E + 00

In order to perform the fatigue analysis, the current is assumed to be constant all year round. The significant results of the VIV analysis are the root mean square (RMS) vibration amplitude and the fatigue life due to bending stresses. In this particular case, we obtained:

– maximum RMS amplitude: 0.59 m at 697 m from top;
– minimum fatigue life: 145 years at 704 m from top.

As can be seen from Figure 2 the amplitude is dominated by mode 3, which is the most energetic mode. Nonetheless, the most dangerous mode for fatigue calculation is the seventh. Its frequency is more than twice the frequency of mode 3, which doubles the number of fatigue cycles per year. Also the curvature of the modal shape associated with the higher mode is larger, creating greater stress.

The maximum fatigue is located in the bottom part of the riser, due to the varying tension along the riser. For a given mode, the nodes are less spaced out near the sea floor, leading to higher stress and fatigue.

2.2.2 Steel Catenary Riser

A steel catenary riser is pinned at the seafloor and tensionned at the top *(Figure 3)*. Its length is 1200 m, the water depth is 1000 m. The diameter is constant at 0.533 m, the current is perpendicular to the riser and its characteristics are given in Table 4.

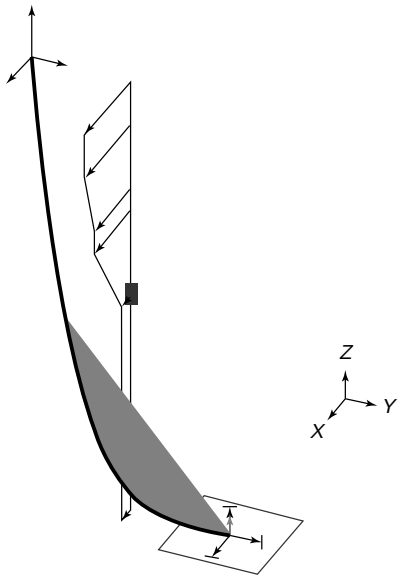

Figure 3

Steel catenary riser with current perpendicular to the structure. The lines linking the structure to the node on the sea-floor represents the nodes which are checked against the bottom of the ocean.

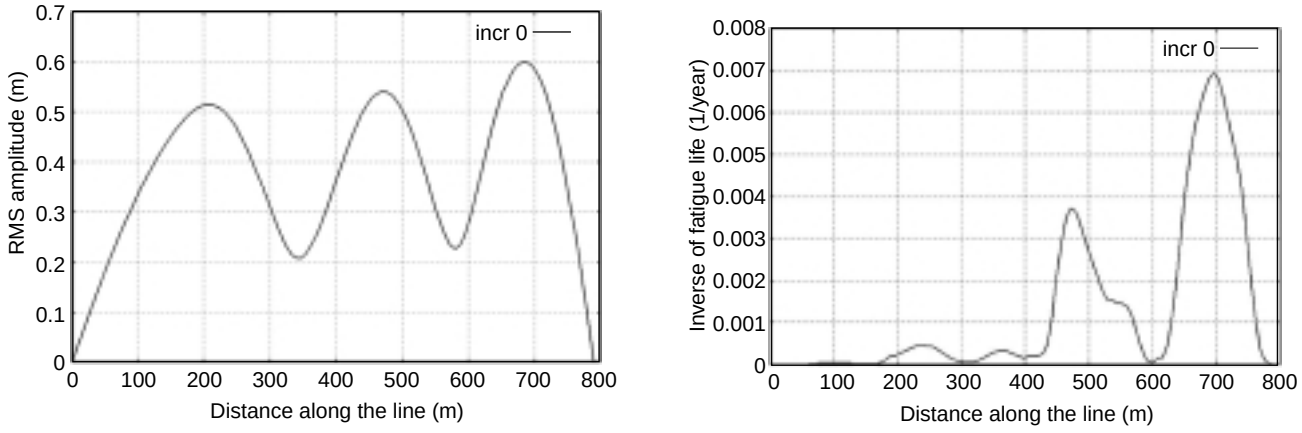

Figure 2

Amplitude and inverse of fatigue life of a drilling riser. The amplitude of vibration is dominated by mode 3 while the most dangerous mode (fatigue) is mode 7.

TABLE 4

Variation of current velocity with depth

Depth (m)	Velocity (m/s)
0	0.5
100	0.5
250	0.4
300	0.4
500	0.1
1000	0.1

The bending mode in the cross-flow direction are automatically selected by the code. The excited eigenfrequencies with $St = 0.2$ are shown in Table 5.

TABLE 5

Excited eigenfrequencies of the steel catenary riser

Mode	Frequency (Hz)
3	0.494E – 01
4	0.713E – 01
5	0.927E – 01
6	0.114E + 00
7	0.136E + 00
8	0.159E + 00
9	0.182E + 00

The results from the VIV analysis are:
- maximum RMS amplitude: 71E-01 m at 983 m from the top;
- minimum fatigue life: 66 years at 1100 m from the top.

In order to increase the life expectancy, VIV suppression devices modeled with an efficiency of 80% are introduced on the first 420 m from the riser top. It implies that the existing force applied on the structure at the top of the riser is reduced by a factor 5.

With VIV suppression devices, we obtain:
- maximum RMS amplitude: m 0.93E – 02 m at 803 m;
- minimum fatigue life: 0.23E + 06 years at 1100 m.

The amplitude and fatigue along the riser are given in Figure 4 for the case with anti-VIV devices. The graphs indicate that, even if the amplitude of vibration is large on the whole length of the riser, the fatigue is located near the touch-down point. The modal curvature in this area is much higher than in the rest of the pipe, the nodes of the mode being more concentrated. The main effect of anti-VIV devices in the area of maximum current velocity is to reduce the vibration of the high modes (bending mode 8 and 9 in our case), which are the most dangerous for the fatigue life.

2.2.3 Remarks

The modal approach gives a good estimate of the fatigue life and allows to study a wide range of cases quickly. Nonetheless, the shortcomings of the methods are the following:
- It is limited to cross-flow vibrations (but in-line forcing could also be introduced).
- It requires bending modes perpendicular to the current. This is always the case for a drilling riser since each bending mode is defined in any direction perpendicular to the normal of the riser section, due to the symmetry of the configuration. The modal basis is in fact composed of pairs of eigenvectors with the same frequency. For more complex geometries (steel catenary riser, export lines, etc.) computations have to be performed with a current in or out of the plane of the structure.

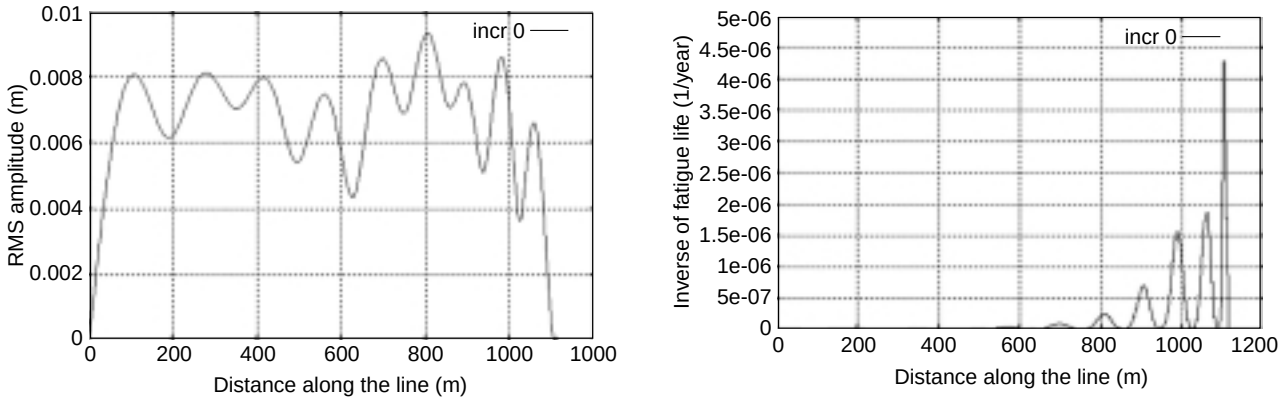

Figure 4

Amplitude and inverse of fatigue life in a steel-catenary riser with anti-VIV devices on the first 420 m. The maximum damage is located in the touch-down area, located at about 1100 m on the plot.

– The current must be steady, therefore wave-effect or top motion cannot be taken into account. An extension of the method to unsteady current is possible (Le Cunff *et al.*, 1999), provided that the modes are not affected by the motion.
– Even for a steady current, the frequencies and phases can evolve in time. To describe such a phenomenon, a more refined fluid model is required.
– The various codes based on a modal approach depend on empirical coefficients and can predict different amplitude on a similar case (see for instance Larsen and Halse, 1995).

3 REFINEMENT OF THE FLUID CALCULATIONS

3.1 Fluid Modeling

3.1.1 Review of the Models

The objective of a fluid model consists of reproducing the force exerted by the fluid on the structure and the way it is influenced by the motion of the structure. From a structural point of view, no detail analysis is required in the description of the fluid. Therefore, the effort should be concentrated on a single parameter (force coefficient) describing the fluid. Obviously, the model should be more refined than the coefficient function of amplitude and *Re* number used in the modal analysis. The model is solved in time, since, even for a steady current, the phenomena are time-dependent.

Several authors defined models where a classical beam equation is solved together with a forcing due to the fluid. For instance, Triantafyllou and Grosenbaugh (1995) proposed a lift coefficient function of the instantaneous amplitude of vibration, lift coefficient which can become a damping force if the amplitude is large, to describe the self-damping mechanism of VIV. Ferrari and Bearman (2000) have a model of the in-line and cross-flow loadings with a Morison type formulation. Guaita *et al.* (2001) use a spring/damper model at each node of the riser to reproduce the fluid behaviour. All these approaches neglect the fluid interactions along the axis. The span-wise coupling of the different fluid forces is therefore effective only through the structure.

Hartlen and Currie (1970) used an oscillator to model the fluid force and its coupling with the structure motion for an elastically supported cylinder. The main idea is to define a differential equation for the lift coefficient which would be characteristic of the fluctuating structure of the near wake. A review of the various equations proposed can be found in Facchinetti (2001).

3.1.2 A Three-Dimensional Approach

The idea of a wake oscillator as first developed by Hartlen and Currie (1970) is based on a phenomenological flow model that summarizes the fluctuating nature of the vortex street by a single variable, governed by a weakly nonlinear Van der Pol's Equation. The fluid variable is the lift coefficient C_L, and the coupled fluid-structure interaction in two dimensions is described by the following equations:

$$\begin{cases} M\ddot{y} + R\dot{y} + Ky = \frac{1}{2}\rho_{\text{flu}} U^2 D L C_L \\ \ddot{C}_L + (-\alpha\omega_{\text{vor}}\dot{C}_L + \frac{\gamma}{\omega_{\text{vor}}}\dot{C}_L^3) + \omega_{\text{vor}}^2 C_L = \beta\dot{y} \end{cases} \quad (5)$$

where the dot denotes a time-derivative and we used the following variables:

y	position of the structure
M, R, K, D, L	mass, damping, stiffness, diameter and length of the structure
β	linear coupling coefficient
ω_{vor}	Strouhal circular frequency
ρ_{flu}, U	fluid density and in-coming flow velocity
α, γ	coefficients characterizing the nonlinearity of the oscillator, α deals with the self-excitation at low amplitude motion and γ with the saturation of large amplitude motion.

This elementary oscillator provides a self-sustained, stable and nearly harmonic oscillation, and is naturally associated with the fluctuating lift proposed by the fluid to the structure. The structure, forced by this improved lift model, interacts on the wake oscillator by means of its displacement and its derivatives. Such a model has been developed for VIV of an elastically supported rigid structure, successfully describing their main features, namely lock-in, qualitatively and even quantitatively. The pioneering work of Hartlen and Currie has been improved by several authors: for a historical review, see Sarpkaya (1979). Comparing to CFD models, this approach does not provide a complete flow field analysis, only focusing on a description of the fluid as "seen" by the structure. This leads to faster computations, nevertheless, several experimental coefficients need to be properly set and the fluid mechanics arguments invoked in their evaluation are not often convincing.

A wake oscillator has been recently improved by Balasubramanian et Skop (1996) in order to model cellular vortex shedding in sheared flow. When a stationary structure experiences a sheared current, spanwise vortex shedding frequency is observed as a step-like function *(fig. 5)*, leading to vortex cells of constant frequency with frequency jumps between them. In the proposed model, a series of wake oscillators are distributed along the spanwise extent of the structure and interact themselves by diffusion, reproducing qualitatively and quantitatively the intrinsic fluid interactions occurring in the near wake, as computed in Figure 6. Spanwise distribution *(z)* of the power spectral density (PSD) associated with the fluid variable clearly shows a cellular vortex pattern.

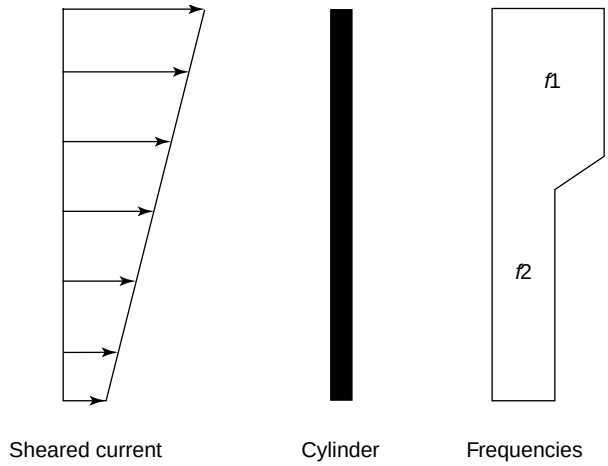

Figure 5

Sketch of the lock-in regions behind a fixed cylinder in a sheared current.

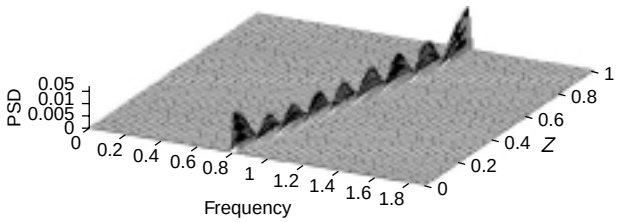

Figure 6

Diffusive coupled Van der Pol oscillators: cellular vortex shedding is evident from the spanwise distribution of the power spectral density (PSD) ossociated to the fluid variable.

The dynamic analysis will provide the vibration amplitude of the riser. In order to determine the fatigue life of the pipe, a rainflow algorithm (for instance Lalanne, 1999) has to be linked to the calculations, requiring a rather large simulation time. But, the resolution of a two-equations model is fast, therefore such method should be of interest for design applications.

3.2 Navier-Stokes Calculations

3.2.1 Description of the Method

The most advanced approach is a computation of the coupled problem, with the beam equation for the structure and the full three dimensional Navier-Stokes equations for the fluid, at very large *Re* (up to 10^6). A numerical simulation by Lucor *et al.* (2001) was conducted on a flexible structure in a sheared flow at *Re* of order 10^3 and aspect ratio (length/diameter) of about 10^3. The computer-time required is still too large to provide a useful tool for design.

Therefore, another alternative consists of computing the Navier-Stokes equations in slices, neglecting the direct influence between the different slices. The three-dimensionality of the problem is taken into account through the riser, and no empirical coefficient is required. In order to approximate the 3D fluid calculations with less computer resources, additional terms can be introduced to link the slices (Willden and Graham, 2000).

In the present paper, a two-dimensional method by slice (Étienne *et al*., 2001) is used to compute the response of a riser. The calculations are performed using DeepLines, the Navier-Stokes solver as well as the coupling procedure defining the module DeepFlow of this code. A specific numerical method has been developed to solve the fluid problem for an arbitrary array of cylinders. A domain decomposition is introduced (Étienne 1999, Étienne *et al.* 1999). In the inner domain, surrounding the cylinders, the two dimensional Reynolds averaged Navier-Stokes equations are formulated based on vorticity (ζ) and stream function (ψ). The turbulent effects are computed with a *k*-ω model. Introducing the turbulent viscosity ν_t and the vector $\boldsymbol{k}$ perpendicular to the 2D slice, the equations are:

$$\begin{cases} \dfrac{\partial \zeta}{\partial t} + (\mathrm{rot}(\psi k)\cdot \mathrm{grad})\zeta = (\nu + \nu_t)\Delta\psi \\ \Delta\psi = -\zeta \end{cases} \qquad (6)$$

In the outer domain, a Lagrangian method is used where particles are convected with a fast vortex method. A coupling procedure takes the position and velocity of the structure as input to the fluid code, which computes the resulting flowfield. The external loads provided by the fluid simulation are then imposed on the structure to reevaluate the position and velocity. This procedure is repeated until convergence at each time step.

3.2.2 Effect of Top Motion on the VIV

A riser in a uniform current at 0.5 m/s is considered with the following characteristics:

- length: 300 m
- external diameter: 0.25 m
- internal diameter: 0.235 m
- linear weight: 157.8 kg/m
- top tension: 1469 kN.

A sinusoidal top motion is imposed with amplitude *A* and circular frequency ω. The relative fluid velocity experienced by the riser at the top is in the range $[U - A\omega, U + A\omega]$. We imposed A = 0.5 m, $A\omega$ = 0.4 and 0.3, leading to periods of 7.9 s and 10.5 s. For a Strouhal number of 0.2, the uniform flow is exciting a frequency of 0.4 Hz, the frequency range with top motion $A\omega$ = 0.4 is [0.08; 0.72]. The first modes of the structure are presented in Table 6.

TABLE 6

The first eight eigenfrequencies of the riser

Mode #	Frequency (Hz)	Period (s)
1	0.09	11.11
2	0.18	5.53
3	0.27	3.67
4	0.36	2.74
5	0.46	2.18
6	0.55	1.78
7	0.66	1.52
8	0.76	1.31

Therefore the first seven modes of the structure are potentially excited when the top motion is imposed. The numerical simulation is performed with forty slices. A snapshot of the riser together with the fluid vorticity in the slices is presented in Figure 7.

In Figure 8, the amplitude of vibration in the cross-flow direction is plotted along the length of the riser. The case $A\omega = 0.4$ exhibits a decrease in the vibration amplitude. For a uniform flow, the structure can impose its frequency to the fluid, creating a lock-in with a large amplitude of vibration. If the current is time-dependant, the lock-in is destabilized, and the vibration tends to decrease. Similar results have been obtained for a cable with a time-dependant modal approach (Le Cunff *et al*., 1999).

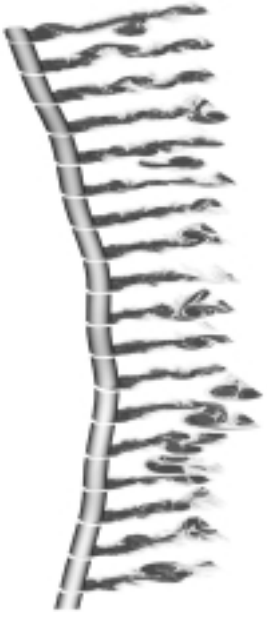

Figure 7

Snapshot of the riser and the fluid slices at t = 40 s, only half the slices are presented.

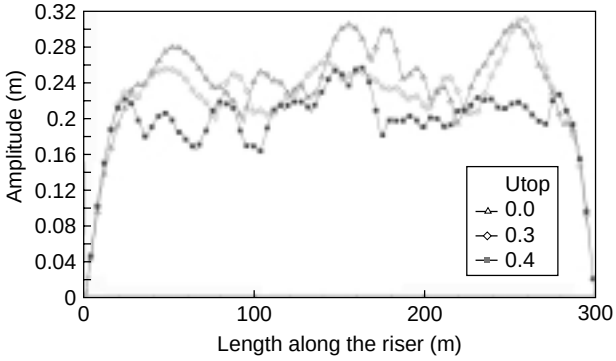

Figure 8

Amplitude of vibration with and without top motion.

4 MEASUREMENTS

A project for the acquisition of VIV data was launched in 1998 entitled "Hydlines", with the financial support of the *Comité d'études pétrolières et marines (CEPM)* as well as the *Club pour les actions de recherche sur les ouvrages en mer (CLAROM)*, and the participation of several companies (*Principia R.D., Doris Engineering, Sirenha, Stolt Offshore, TotalFinaElf)* together with *Institut français du pétrole* and *École supérieure des ingénieurs de Marseille.* The objectives were to obtain large Reynolds data on a towed cylinder, to study the effect of anti-vibration devices, and finally to observe a multimodal response for a cable. In this paper, we will present the latter part of the project.

4.1 Experimental Setting

The experiments were carried out at the "bassin de génie océanique First" (BGO First) in La Seyne-sur-Mer. The basin has a useful testing area of 24 × 16 m. The maximum speed velocity is 0.5 m/s. The depth is adjustable up to 5 m. A conceptual study was conducted by Molin (1999) and Le Cunff (1999) to define the geometry and observable frequencies. Results for each configurations were monitored during the experiments to verify their accuracy (Pluvinet, 1999).

A 3 m depth is used, with a velocity ranging from 0.2 to 0.4 m/s. The cable is fixed at the bottom of the basin and tensioned at the top. *(Fig. 9).*

The cable has the following characteristics:

– length between the fixed point and the pulley: 20.9 m
– diameter: 0.5 mm
– mass: 0.103 kg/m
– tension: between 200 N and 800 N.

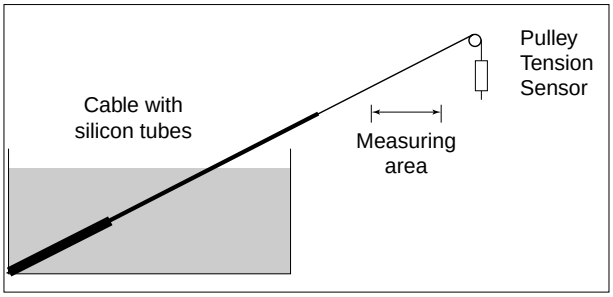

Figure 9

Sketch of the experimental setting.

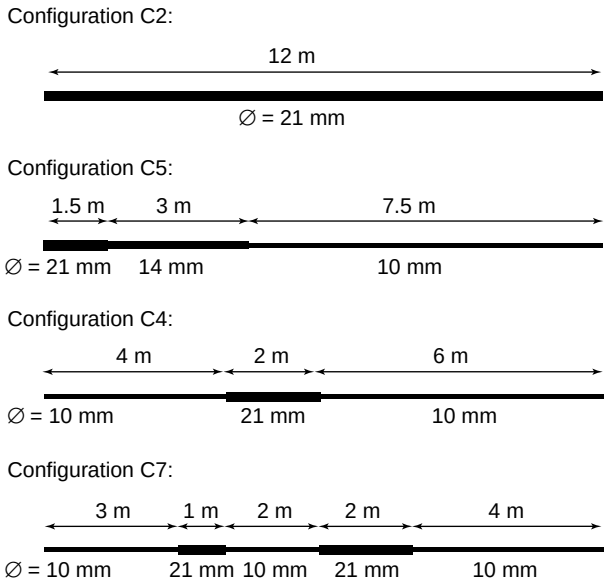

Figure 10

Examples of cable configuration.

4.2 Experimental Results and Comparisons

Various cable configuration were studied and four of them are represented in Figure 10. The first one (C2) has a constant diameter in water, the second one (C5) has three diameters and the third one (C7), two diameters. The first 12 m of cable, starting from the fixed point, are indicated. The rest of the structure is the bare cable with a 5 mm diameter.

The Reynolds number for all the cases considered is less than 10^4. Measurements to verify the accuracy of the incoming flow velocity along the cable were conducted by Kimmoun *et al.* (2000) for three different positions.

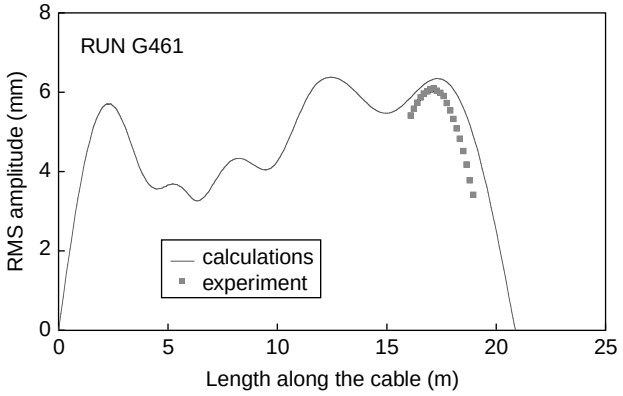

Figure 11

Comparison between DeepVIV and experimental results for the RMS amplitude of vibration.

Comparisons with DeepVIV are presented in Figure 11 on configuration C4 with a top tension of 800 N and a current velocity requirement of 0.4 m/s. The RMS amplitude of vibrations in the cross-flow direction is plotted along the cable length. It shows that the agreement is very good in the case of multi-modal excitation.

CONCLUSION

A review of the work conducted at *Institut français du pétrole* in collaboration with *École supérieure des ingénieurs de Marseille* and *École polytechnique* on vortex-induced vibrations is presented. Several approaches are studied in order to provide a reliable method to compute the fatigue life of risers submitted to currents. The range extends from a simple modal approach to Navier-Stokes calculations. A "middle of the road" technique is developed based on the time-dependant solution of the structural equation coupled with a model equation for the fluid forcing. It is expected that such a method will provide a powerful tool for riser design.

Detailed experiments have also been conducted in collaboration with industrial partners to gather data on a wide range of configurations. They provide benchmarks test for the various numerical tools at our disposal.

ACKNOWLEDGEMENTS

We would like to acknowledge the financial support of the *CEPM* and *CLAROM* through grant M.02117/98 and M.7502/99. The Hydlines project included the following *CLAROM* members: *Principia R.D., Institut français du pétrole, Doris Engineering, École supérieure des ingénieurs de Marseille, Sirenha, Stolt Offshore, TotalFinaElf*. The model tests at BGO First were made possible by funding

from the Hydlines project's members. These tests were carried out under The *GISHYDRO* research program with a partial financial support from Conseil général du Var. Finally, we would like to thank the partners of the Hydlines project for permission to publish a comparison with experimental results.

REFERENCES

Balasubramanian, S. and Skop, R. A. (1996) A Nonlinear Oscillator Model for Vortex Shedding from Cylinders and Cones in Uniform and Shear Flows. *J. of Fluids and Structures*, **10**, 197-214.

Bearman, P.W. (1984) Vortex Shedding from Oscillating Bluff Bodies. *Ann. Rev. Fluid Mech*., **16**, 195-222.

Blevins, R.D. (1990) *Flow-Induced Vibration*, Van Nostrand Reinhold, Co.

Bokaian, A. (1993) Lock-in Prediction of Marine Risers and Tethers. *J. Sound and Vibrations*, **175**, 607-623.

Bruschi, R., Jacobsen, V., Simantiras, P. and Vitali, L. (1996) Vibration Suppression Devices for Long, Slender Tubulars. *Proc. OTC*, 71-80.

Chen, S.S. (1987) *Flow Induced Vibration of Circular Cylindrical Structures*, Hemisphere Publishing Corp., Springer-Verlag, Chap 7.

DeepLines™ (2000) Keywords Manual, *IFP/PRD Report V2r2.*

DNV (1996) *Rules for Submarine Pipeline Systems*, Section 5, C509/C510.

Étienne, S., Scolan, Y.M. and Biolley, F. (1999) Modélisation numérique de l'écoulement de fluide visqueux autour d'un faisceau de riser. *7e Journées de l'hydrodynamique*, Marseille, France, 57-72.

Étienne, S. (1999) Contribution à la modélisation de l'écoulement de fluide visqueux autour de faisceaux de cylindres circulaires. *Thèse de doctorat de l'université de la Méditerranée*, Aix - Marseille II - École supérieure d'ingénieurs de Marseille.

Étienne, S., Biolley, F.,. Fontaine, E., Le Cunff, C. and Heurtier, J.M. (2001) Numerical Simulations of Vortex Induced Vibrations of Slender Offshore Structure. *Proc. of ISOPE Conference*, **3**, 419-425.

Every, M.J., King, R. and Weaver, D.S. (1982) Vortex-Induced Vibrations of Cylinders and Cables and their Suppression, *Ocean Engineering*, **9**, 135-157.

Facchinetti, M.L. (2001) Vibrations induites dans les courants non uniformes. *Rapport IFP* n° 55815.

Ferrari, J.A. and. Bearman, P.W (2000) A Three-Dimensional Model for Wave and Vortex-Induced Vibration of Deepwater Riser Pipes. *Flow-Induced Vibrations*, 3-10.

Guaita, P., Fossati, F. and Resta, F. (2001) Development and Test of a Time-Domain VIV Prediction Model. *Proc. of Offshore Mediterranean Conference*, Paper No 61.

Griffin, O.M. (1985) Vortex-Shedding from Bluff Bodies in a Shear Flow: a Review. *Transactions of the ASME*, 298-306.

Hartlen, R.T. and Currie, I.G. (1970) Lift-Oscillator Model of Vortex-Induced Vibration. *J. of the Engineering Mechanics Division*, 577-591.

Hopper, C.T (1983) Vortex-Induced Oscillations of Long Marine Drilling Risers. *Proc. of DOT*, 97-109.

Huse, E., Kleiven, G. and. Nielsen, F.G (1998) Large Scale Model Testing of Deep Sea Risers. *Proceedings of OTC*, 44-61.

Iwan, W.D. (1981) The Vortex-Induced Oscillations of Nonuniform Structural Systems. *J. of Sound and Vibrations*, **79**, 291-301.

Kimmoun O., Molin, B. and Zucchini, B. (2000) Mesures par film chaud de la vitesse du courant dans le bassin de génie océanique First. *Rapport ESIM* du 27 mars 2000, Projet CLAROM HydLines.

Lalanne, C. (1999) *Vibrations et chocs mécaniques*, Hermès Science Publication, Paris.

Larsen, C.M. and. Halse, K.H (1995) Comparison of Models of Vortex Induced Vibrations of Slender Marine Structures. *Flow Induced Vibrations*, 467-482.

Le Cunff, C. (1999) Note de calculs sur les essais 3D. *Note externe IFP* n° I4455066-1.

Le Cunff, C., Biolley, F. and Durand, A. (1999) Prediction of the Response of a Structure to Vortex-Induced Vibrations: Comparison of a Modal and a Wave Aproach. *Proc. 18th OMAE Conference*, St John's, Canada, 1-8.

Lucor, D., Imas, L. and Karniadakis, G.E. (2000) Vortex Dislocations and Force Distribution of Long Flexible Cylinders Subjected to Sheared Flows. *J. Fluids and Structure*, **15**, 641-650.

Lyons, G.J. and Patel , M.H. (1989) Application of a General Technique for Prediction of Riser Vortex-Induced Response in Waves and Current. *J. of ASME*, **111**, 82-91.

Marris, A.W. (1964) A Review on Vortex Sreets, Periodic wakes, and Induced Vibrations Phenomena. *J. of Basic Eng*., 185-196.

Moe, G. (1991) An Experimentally Based Model for Prediction of Lock-in Riser Motions. *Proc. of OMAE Conference*, **1-B**, 497-506.

Molin, B. (1999) *Personal Communication.*

Morison, J.R., O'Brien, M.P., Johnson, J.W. and Schaaf, S.A. (1950) The Forces Exerted by Surface Waves on Piles. *Petroleum Trans., AIME*, **189**, 149-157.

Naudascher, E. (1987) Flow-Induced Streamwise Vibrations of Structures. *J. of Fluids and Structures*, **1**, 265-298.

Naudascher, E. and Rockwell, D. (1994) *Flow-Induced Vibrations – An Engineerin Guide*, Balkema A.A.

Nedergaard, H., Ottesen Hansen, N.-E. and Fines, S. (1994) Response of Free Hanging Tethers. *Proc. of BOS 94*, 315-332.

Pantazopoulos, M.S. (1994) Vortex-Induced Vibrations Parameters: Critical Review. *Proc. of OMAE*, **1**, 199-255.

Pluvinet**,** F. (1999) HydLines essais 3D : rapport d'essais, *Document Principia, n° RET*.95.304.01.

Sarpkaya, T. (1979) Vortex-Induced Oscillations - A Selective Review. *J. of Applied Mech*., **46**, No. 2.

Sheppard, R.M. and Omar, A.F. (1992) Vortex-Induced Loading on Offshore Structures: a Selective Review of Experimental Work. *Proc.of OTC*, 183-112.

Torum, A., Moe, G., Johansen, J.V and Katla, E. (1996) On Current Induced In-Line Oscillation in Pipelines Free-Spans. *Proc. of OMAE Conference*, **5**, 459-469.

Triantafyllou, M.S. and Grosenbaugh, M.A. (1995) Prediction of Vortex-Induced Vibrations in Sheared Flow. *Flow-Induced Vibrations*, Bearman (Ed.) Rotterdam.

Vandiver, J.K. (1987) The Relationship between In-Line and Cross-Flow Vortex-Induced Vibration in Cylinder. *J. of Fluids and Structures*, **1**, 381-399.

Willden, R.H.J. and. Graham, J.M.R (2000) Vortex Induced Vibrations of Deep Water Risers. *Flow-Induced Vibrations*, 29-36.

Williamson, C.H.K. (1996) Vortex Dynamics in the Cylinder Wakes. *Ann. Rev. Fluid Mech*., **28**, 477-539.

Zdravkovich, M.M. (1981) Review and Classification of Various Aerodynamic and Hydrodynamic Means for Suppressing Vortex Shedding. *J. Wind Eng. And Industrial Aerodynamics*, **7**, 145-189.

Final manusvript received in October 2001